



**New Jersey Geological Survey
Geological Survey Report 17**

**GEOPHYSICAL INVESTIGATIONS TO DETERMINE
BEDROCK TOPOGRAPHY IN THE
EAST HANOVER-MORRISTOWN AREA, MORRIS COUNTY, NEW JERSEY**



STATE OF NEW JERSEY

Thomas H. Kean, *Governor*

Department of Environmental Protection

Christopher J. Daggett, *Commissioner*

Division of Water Resources

Eric Evenson, *Acting Director*

Geological Survey

Haig F. Kasabach, *State Geologist*

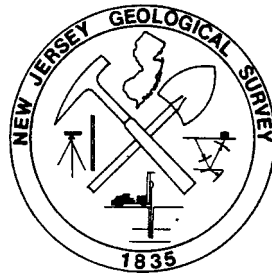
Cover photo: Ford House, Washington's Headquarters 1779-80.

With access from the west blocked by the rugged granitic hills of the New Jersey Highlands and routes from the north, east and south guarded by the Watchung basalt ridges and marshlands developed above the sediments of glacial Lake Passaic, Morristown was an ideal location for overwintering, easily defended and close enough to monitor British activities in New York City. Washington twice took advantage of this strategic location, overwintering at Morristown through 1776-77 and 1779-80.

**New Jersey Geological Survey
Geological Survey Report 17**

**GEOPHYSICAL INVESTIGATIONS TO DETERMINE
BEDROCK TOPOGRAPHY IN THE
EAST HANOVER-MORRISTOWN AREA, MORRIS COUNTY, NEW JERSEY**

by
Suhas L. Ghatge and David W. Hall



New Jersey Geological Survey Reports (ISSN 0741-7357) are published by the New Jersey Geological Survey, CN-029, Trenton, NJ 08625. This report may be reproduced in whole or part provided that suitable reference to the source of the copied material is provided.

Additional copies of this and other reports may be obtained from:

Maps and Publications Sales Office
Bureau of Revenue
CN-402
Trenton, NJ 08625

A price list is available on request.

Use of brand, commercial, or trade names is for identification purposes only and does not constitute endorsement by the New Jersey Geological Survey.

CONTENTS

	page
Abstract	1
Introduction	1
Acknowledgments	1
Geology	2
Previous investigations	3
Geophysical field methods	3
Gravity	3
Seismic refraction	3
Electrical resistivity and induced polarization	3
Geophysical data reduction and interpretation	4
Gravity	4
Seismic refraction	9
Electrical resistivity and induced polarization	9
Summary and conclusions	11
References	12

FIGURES

Figure 1. Location of the study area and regional geology	2
2. Gravity profile A-A' and interpreted depth section (with all wells)	5
3. Gravity profile A-A' and interpreted depth section (without two wells)	6
4. Gravity profile B-B' and interpreted depth section	7
5. Gravity profile C-C' and interpreted depth section	8
6. Seismic refraction travel time curve with interpreted depth section for Line EH-2	10
7. Electrical resistivity-R) sounding EHVES-2 with interpretation.....	11

PLATES

(in pocket)

Plate I. Bouguer gravity anomaly map	
II. Residual gravity anomaly map	
III. Bedrock topography map	

APPENDIX

Table	1. Principal facts of gravity stations.....	17
	2. Seismic refraction field parameters and interpretation	20
	3. Electrical resistivity and IP soundings and interpretations	23
	4. Records of wells	24

GEOPHYSICAL INVESTIGATIONS TO DETERMINE BEDROCK TOPOGRAPHY IN THE EAST HANOVER-MORRISTOWN AREA, MORRIS COUNTY, NEW JERSEY

by

Suhas L. Ghatge and David W. Hall

ABSTRACT

Gravity, seismic refraction, electrical resistivity, and induced polarization methods were used to determine bedrock topography in the East Hanover-Morristown area of Morris County, New Jersey. Previous investigations, based on well information and seismic refraction surveys, had identified parts of the East Hanover buried valley system, but not in sufficient detail for ground-water pollution investigations.

A residual gravity anomaly map generated from a Bouguer anomaly map by the removal of the regional gravity (represented by a first degree double Fourier series trend surface) shows the East Hanover buried valley and the northern extension of the Chatham buried valley.

Two-dimensional inverse modeling of three gravity profiles adequately resolves the depth to bedrock along the profiles. Interpretation of 22 seismic refraction lines, 3 out of 6 electrical resistivity-induced polarization soundings, and well logs provided bedrock depths at spot locations. A bedrock topography map was prepared using all the geophysical and well data. This map has been utilized in ground-water pollution studies of the area to show ground-water flow.

INTRODUCTION

This geophysical investigation was carried out to assist in the investigation of ground-water pollution in the East Hanover-Morristown area (fig. 1), Morris County, New Jersey. The major pollutants are volatile organic compounds (Oudijk, 1987). A single source of the contamination has not been determined but there are several industries in the area which may be sources.

Direct detection of contaminated ground-water was not possible using geophysical techniques because of the low concentrations of contaminants. However indirect study seemed possible because the bedrock surface is believed to influence the local ground-water flow.

Four surface geophysical methods were integrated with depth-to-bedrock data from well records and results of previous geophysical investigations to determine the topography of the bedrock surface. The geophysical methods were gravity, seismic refraction, electrical resistivity, and induced polarization.

The choice of methods and placement of stations was severely constrained by the urban character of the study area. Space limitations, buildings and roads, electrical noise from power lines, and acoustic noise from highways and equipment limited quality of data from seismic and electrical methods. Gravity measurements

are effective for buried valley delineation (Hall and Hajnal, 1962; Stewart, 1980), less susceptible to cultural noise than other methods, and require only a small area to take a reading. Therefore, gravity measurements were considered to be the best geophysical method to determine bedrock topography in this area. Gravity data can also be collected with a minimum amount of field time, even though each measurement station has to be surveyed for vertical and horizontal control. The majority of the geophysical data collected in this study was, therefore, gravity data.

Gravity measurements were taken at 131 stations within an area of approximately 20 square miles. In addition, seismic refraction data were collected at 22 locations and six electrical resistivity soundings and three induced polarization soundings were taken.

Acknowledgments

The authors gratefully acknowledge the assistance of Stewart Sandberg, John Groenewold, David Pasicznyk, Thomas Bambrick, James Boyle, and Donald Jagel in collection and interpretation of data and Jeffrey Olson and Joseph Rich for providing the elevations and locations of the gravity stations. The authors also want to thank the authorities of Bell Laboratories, Whippany and Morristown Municipal airport for permission to collect data in their properties.

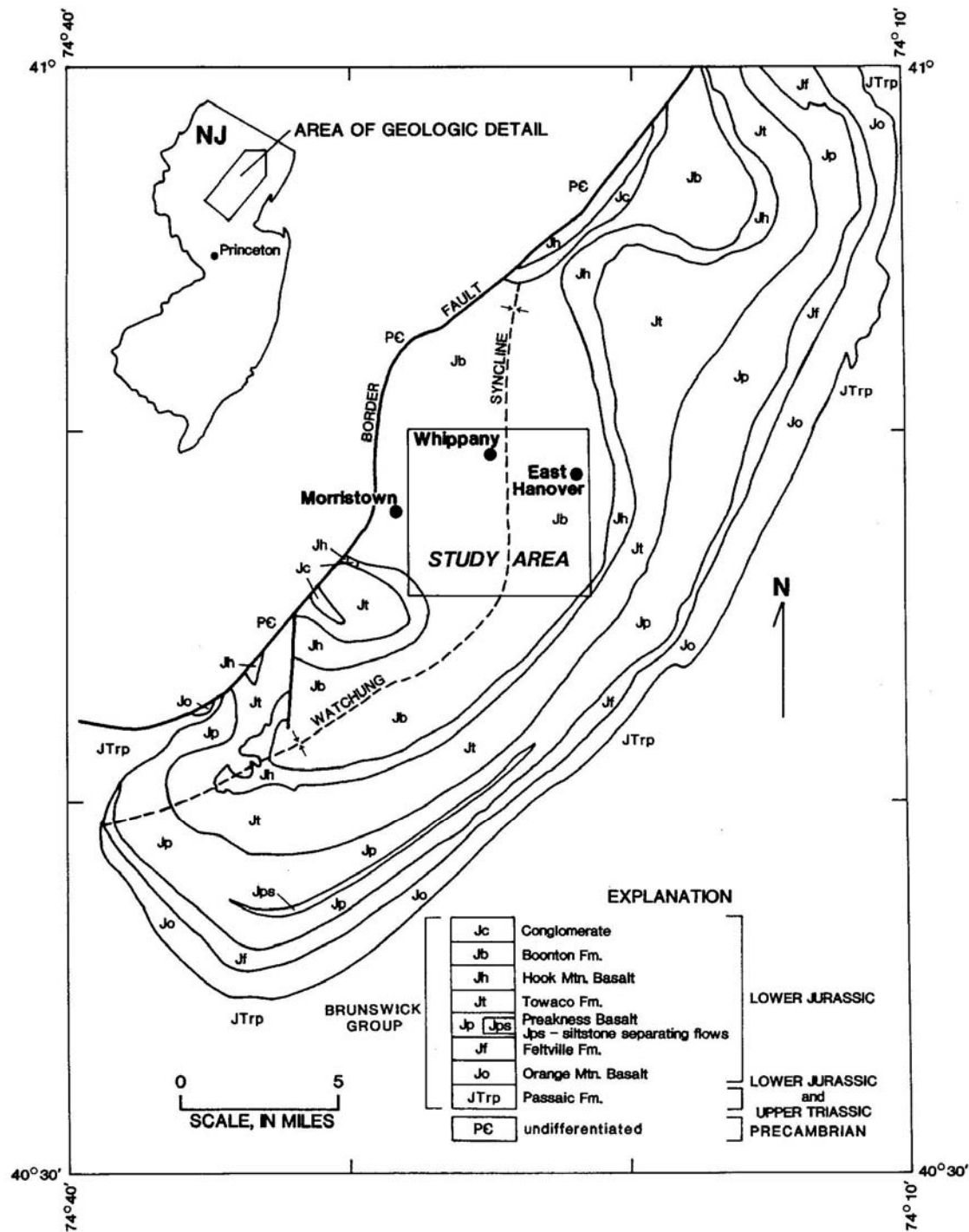


Figure 1. Location of the study area and regional geology.

GEOLOGY

The Boonton Formation, the youngest unit of the Newark Supergroup in New Jersey (Olsen, 1980) forms the bedrock in the study area. The Boonton Formation, part of the Brunswick

Group (Lyttle and Epstein, 1987), consists of about 1640 ft of red, brown, gray, and black, fine to coarse clastics and minor evaporite beds. It overlies the Hook Mountain Basalt (Olsen,

1980), the youngest extrusive rock unit in the Watchung Syncline (fig. 1). There are no bedrock exposures within the study area, but Lyttle and Epstein (1987) show the bedrock beneath the unconsolidated sediment to be rather flat lying, with dips of less than 10 degrees. The Border Fault, west of the study area, separates rocks of the Brunswick Group (fig. 1) from Precambrian gneisses.

Above the bedrock is unconsolidated, valley-filling sediment of Quaternary age. These deposits consist of till, clay, silt, sand, and gravel of glacial, lacustrine, and fluvial origin (Salisbury, 1902; Gill and Vecchioli, 1965). The sediments are predominantly late Wisconsinan tills and lacustrine sediments deposited in glacial Lake Passaic.

GEOPHYSICAL FIELD METHODS

Gravity

The gravity meter used in this study was a Lacoste & Romberg Gravimeter (Model G77) capable of reading to the nearest 0.01 milligal (mGal; 1 mGal = 0.001 cm/s²).

Gravity readings were taken at 131 locations (plate III; table 1, appendix) mainly at benchmarks, road intersections, or along roads. The accuracy of the micrometer readings was maintained by taking successive observations until duplication was obtained to within 2 micrometer divisions (1 micrometer division is about 0.010356 mGal). Counter readings were converted to mGal values according to the gravity meter specifications. Station elevations were obtained by leveling to an accuracy of ± 0.2 ft. Latitudes were obtained from USGS 7.5 minute quadrangle maps and by surveying from benchmarks. The margin of error in latitude was 0.025 minutes. The gravity measurements had an accuracy of ± 0.02 mGal due to instrument, elevation, and latitude accuracy.

The primary base station was that established by Bonini and Woollard (1957) in Guyot Hall, Princeton University, about 32 miles south of the survey area. The observed gravity at the Princeton base station is 980177.6 mGal (Bonini and Woollard, 1957). A secondary base station, EH1, was established at New Jersey Geodetic Control Survey monument no. 5306, located opposite the Washington Monument on Morris Avenue (route 510) in Morristown. A value of 980198.48 mGal was established by repeated loops with the primary base station.

Previous Investigations

Maps showing inferred locations of sediment-filled valleys in the study area are in Salisbury (1902), but little was known at that time as to their exact location or depth. Gill and Vecchioli (1965) used well data and Gill and others (1965) incorporated seismic data in bedrock topographic maps of the area. These were substantially improved by Vecchioli and Nichols (1966), Vecchioli and others (1967), and Nichols (1968). Nichols (1968), using bedrock elevations from wells, test holes, and seismic refraction, identified the East Hanover valley as a separate tributary of the Chatham valley extending from Florham Park into East Hanover Township where it joins the Millburn valley.

Seismic Refraction

Seismic refraction data (table 2, appendix) were collected at 22 locations (plate III) in the East Hanover-Morristown area in the vicinity of the Morristown Municipal Airport. Data were collected using a Bison 8012A, 12-channel, signal enhancement seismograph, and automatically recorded in the field. A 20-ft geophone spacing was used for most lines. A 50-ft spacing was used on lines EH 1 for greater depth penetration. The geophones used were Terra Dynamics ADR-711 accelerometers. Accessibility and the level of background noise dictated which seismic source was used. A trailer-mounted vacuum-actuated weightdrop (E.G.& G. Dynasource) was used at the majority of the shotpoints. An 8- or 10-gauge "Buffalo Gun" was used in remote areas.

Electrical Resistivity and Induced Polarization

Electrical resistivity and induced polarization (IP) sounding data were collected at 3 of the 22 locations where seismic refraction data were collected. Resistivity sounding data (without IP data) were also collected at 3 other seismic refraction traverse sites (plate III; table 3, appendix).

Resistivity and IP data were collected using the Schlumberger configuration (Dobrin, 1976). The Schlumberger electrode array was used with varying maximum current-electrode (AB) spacing. For soundings EHVES-1, EHVES-2, EHVES-3, and EHVES-6, maximum AB spacings were 1312.4 ft; EHVES-4 had a maximum

spacing of 16403 ft; and EHVES-5 had a maximum spacing of 2073.6 ft. Data were obtained using the Hunttec M4 2.5kW resistivity/induced polarization system. Steel stakes were used for transmitting current into the ground. Copper-copper sulfate, porous-pot electrodes were used at the receiver for making the voltage measurements; data were automatically recorded.

Data were collected in response to a transmitted waveform composed of successive two-second intervals each of on-positive, off, on-

negative, and off pulses. Voltage readings at the receiver were obtained during the on-time and for ten windows of 100 milliseconds (ms) width starting 100 ms after turnoff of the transmitted current. The on-time voltage measurements were used to obtain the resistivity data. The induced polarization data consisted of apparent chargeabilities in milliseconds which were obtained by summing the average voltage from each of the ten time windows and then dividing this sum by the average on-time voltage.

GEOPHYSICAL DATA REDUCTION AND INTERPRETATION

Gravity

Data Reduction

Gravity measurements were reduced to simple Bouguer gravity values using formulas in Dobrin (1976). Corrections for tidal effects, instrumental drift, latitude, and elevation were performed using a gravity reduction computer program.

Gravity readings were converted to observed gravity values by correcting for tidal and instrumental drift with base-station readings at intervals of two hours or less. The latitude effect at each station was calculated from the theoretical gravity at sea-level, using the International Gravity Formula of 1930 (Dobrin, 1976). The effect of station elevation above sea-level datum was determined using the free-air and Bouguer corrections. A density of 2.67 gm/cc was used in the Bouguer correction. Terrain corrections, which account for the deviation of topography from a horizontal surface, were calculated at some stations but were not used because they were not significant. Bouguer gravity values were then calculated, plotted, and contoured to obtain a Bouguer gravity anomaly map (plate I).

A residual gravity map (plate II) was prepared from the Bouguer anomaly data using the double Fourier series analysis computer program of James (1966). This program is used for trend surface analysis of irregularly spaced data.

The program removed from the Bouguer gravity values all wavelengths in excess of 4.375 miles in the north-south direction and 6.25 miles in the east-west direction.

Interpretation

The residual gravity map (plate II) shows gravity lows which coincide with parts of East

Hanover buried valley filled with relatively low-density clay and muck. This trend in gravity lows is interrupted by a WNW-ESE trending gravity high located northeast of Morristown Airport. This gravity high may be relatively high-density overburden, possibly till or weathered bedrock, underlying the clay. The trend of gravity lows coincident with the East Hanover buried valley is flanked on the west by a gravity high trending NE-SW indicating a bedrock high.

A gravity low in the southwestern part of the residual gravity map (pl. II) may be due to the low density material within the northern extension of the Chatham buried valley.

For higher-resolution gravity interpretation and depth determination, a two-dimensional, non-linear, least-squares gravity inversion program was used to model the gravity data in profile form. This program incorporates the Marquardt procedure (Beck and Arnold, 1977) to calculate the new model parameters. Three profiles, A-A', B-B' and C-C' (plate I), were modeled using this program.

The gravity field of the initial model was calculated at each station on the surface using the line integral algorithm (Talwani and others, 1959). The initial model consisted of depths to bedrock obtained from well information, seismic refraction, and, in profile B-B', electrical resistivity and IP data. The Hook Mountain Basalt and gneiss west of the Border Fault were included in the models since they contribute to the regional gravity effect. Density contrasts of the various bodies were the fixed parameters in the modeling.

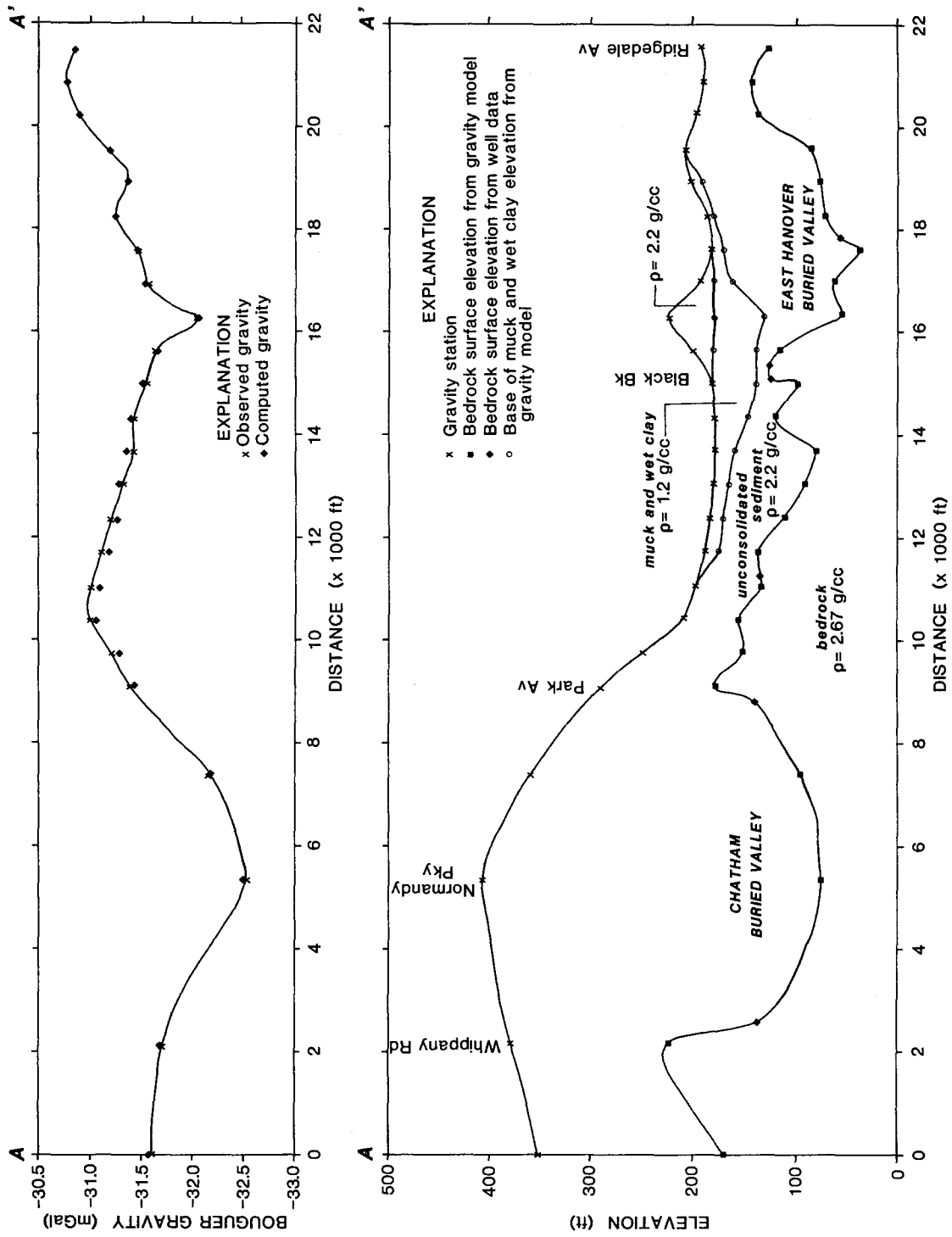


Figure 2. Gravity profile A-A' (top) and interpreted cross section (bottom, with all wells). Location of section shown on plate 1.

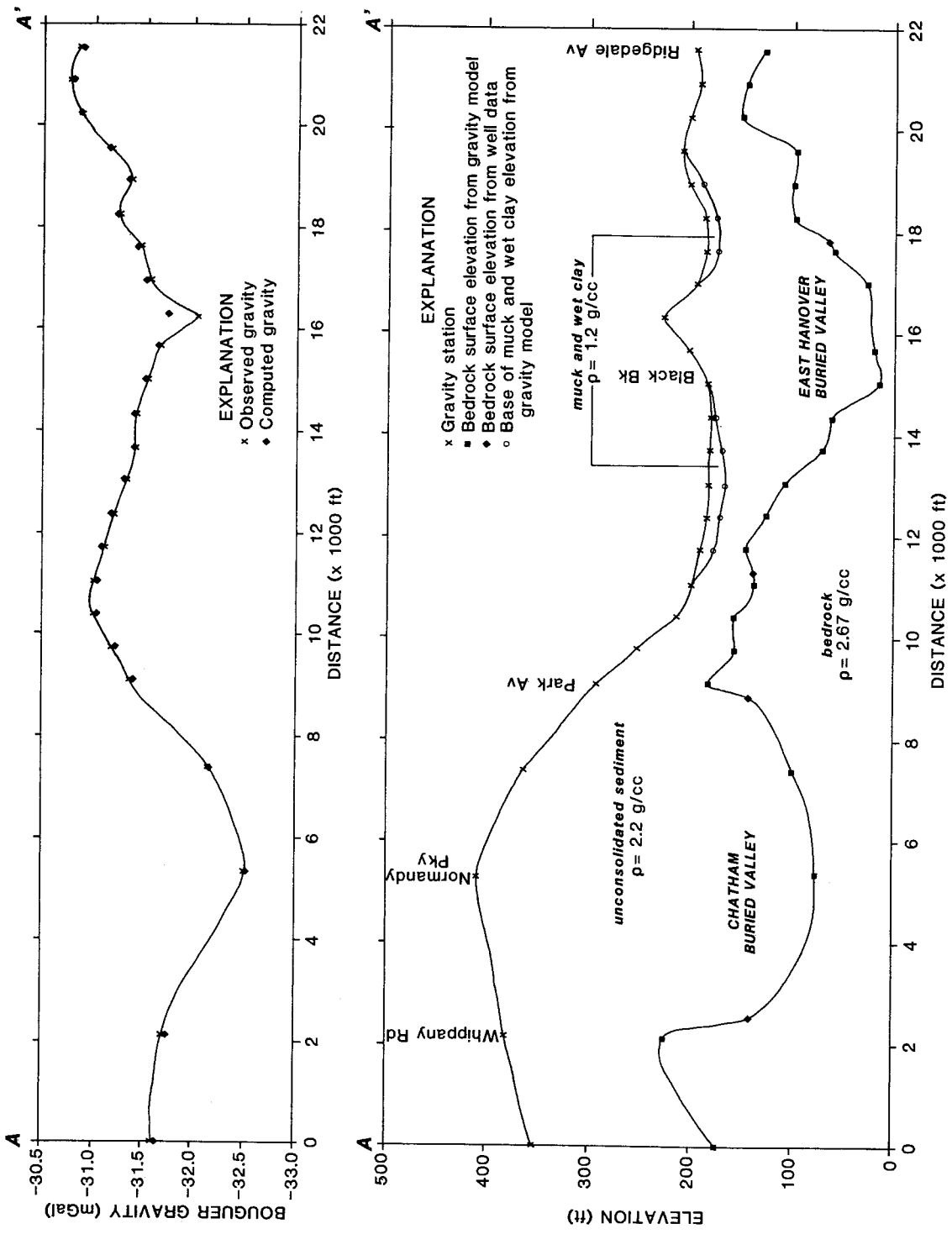


Figure 3. Gravity profile A-A' (top) and interpreted cross section (bottom, without two wells). Location of section shown on plate 1.

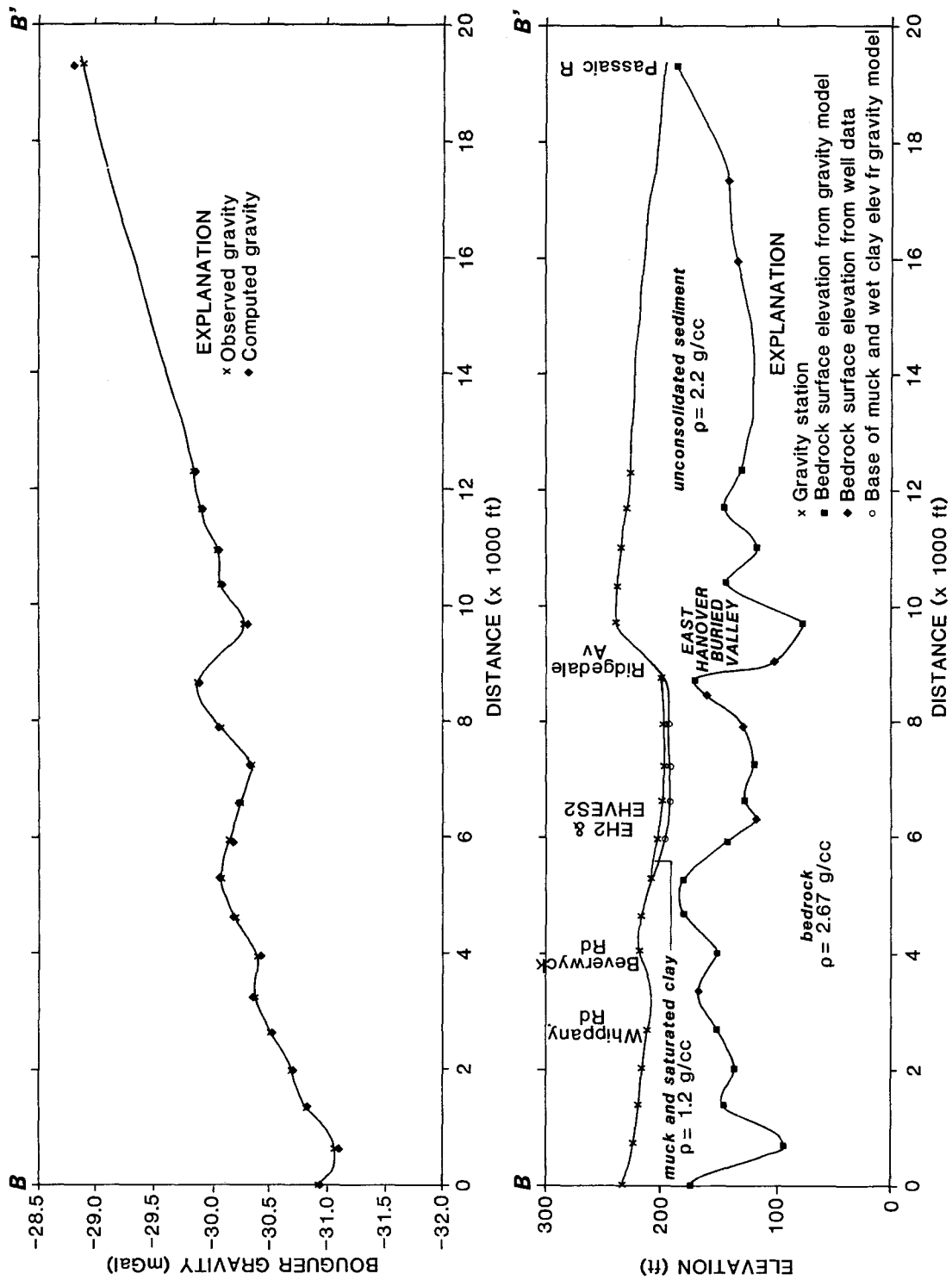


Figure 4. Gravity profile B-B' (top) and interpreted cross section (bottom). Location of section shown on plate 1.

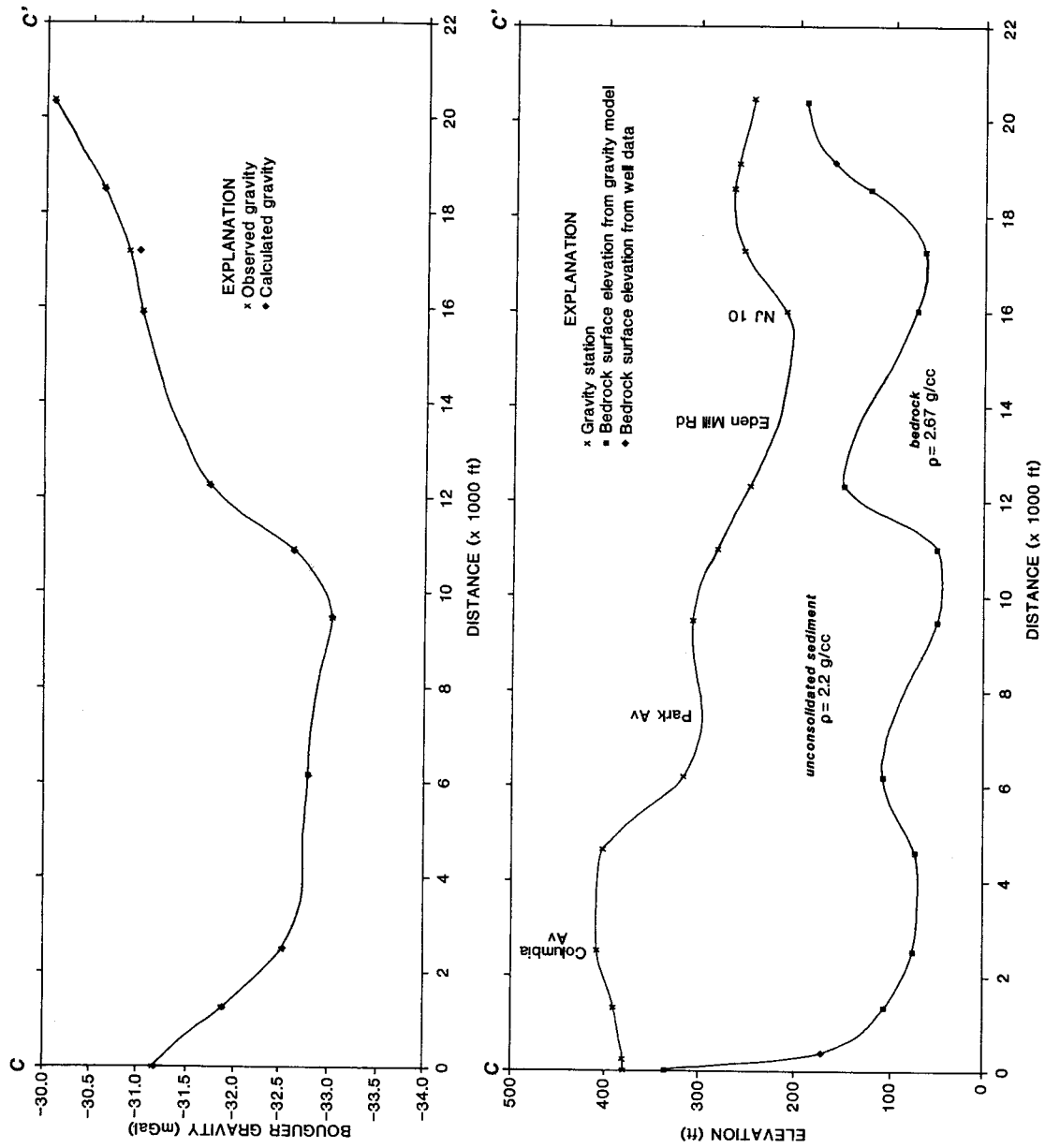


Figure 5. Gravity profile C-C' (top) and interpreted cross section (bottom). Location of section shown on plate 1.

Densities used in the modeling, adapted from Dobrin (1976), Telford and others (1976), and Kodama (1983) are as follows:

Gneiss	2.72 gm/cc
Boonton Formation	2.67 gm/cc
Hook Mountain Basalt	2.96 gm/cc
Saturated clay and muck . . .	1.20 gm/cc
Unconsolidated sediments . .	2.22 gm/cc

Bedrock depths at gravity stations on the profiles were the values that were changed in the modeling process. There are many possible models that would result in the same gravity anomaly, therefore the interpretation of gravity data is ambiguous. Hence, constraints on depths or densities obtained using other methods are essential. Depth at each gravity station was re-calculated when the calculated gravity value did not adequately fit the Bouguer gravity value. When the gravity values from the calculated model fit the observed gravity data with an error of no more than ± 0.02 mGal and the model provided the lowest standard deviation for all parameters it was accepted as the final model.

Interpreted depth sections corresponding to gravity profiles B-B' (fig. 4) and C-C' (fig. 5) are geologically reasonable and data fit is good. Interpretation of gravity profile A-A' (figs. 2, 3) is problematic. In figure 2, bedrock elevations at two wells, located at 15,089 ft and 16,230 ft, are used to constrain the model for profile A-A'. These two wells show bedrock elevations of 125 and 126 ft according to Gill and others (1965) and Nichols (1968), showing a bedrock high in the area. The interpreted depth section from gravity modeling (fig. 2) does not seem to be geologically reasonable in the vicinity of the two wells. In order to raise the bedrock surface of the gravity model to the level of the wells, it was necessary to increase the thickness of the muck and saturated clays in the depth section and extend it beneath denser unconsolidated sediments.

The location of these two wells is questionable. Despite careful search at U.S. Geological Survey, Trenton, and NJ Department of Environmental Protection, Trenton, no records could be found. Accordingly, the gravity profile was reinterpreted without these two bedrock elevations as constraints (fig. 3). The interpreted depth is geologically reasonable and shows the valley to be broader and deeper. Data fit is good except at station EH 22, table 1, possibly due to instrument noise.

Seismic Refraction

The seismic refraction data analysis was performed using the computer programs HRASSD (Hoffman and Waldner, 1986) and SIPT (Scott, 1977). HRASSD was used to pick the time breaks and the corresponding layer numbers for individual shot points. These values were input to the SEPT program of Scott (1977). SIPT was used to calculate average apparent velocities for each layer and then assemble data from several shotpoints from both the forward and reverse traverses into a single profile using the ray tracing algorithm of Scott and others (1972).

Generally, a three-layer model was used in analysis of the refraction data. In the near-surface layer (layer 1) average velocity is between 925 and 2000 ft/s and probably represents the unsaturated overburden. The next layer (layer 2) has an average velocity between 4000 and 7000 ft/s and is probably saturated overburden below the water table. The deepest layer (layer 3) is the shale of the Boonton Formation, with an average velocity between 10,000 and 13,000 ft/s. Figure 6 shows a time-distance curve and interpreted depth section for seismic refraction profile EH 2. The profile itself is shown on gravity profile B-B' (fig. 4). The interface between layer 1 and layer 2 is the water table, which has an average depth of 5.4 ft below surface. The depth below land surface to layer 3 ranges from 46 to 83 ft. Average velocity of layer 3 is 10,200 ft/s. This velocity indicates that the bedrock is probably shale. A well south of the seismic profile shows a bedrock depth of about 100 ft.

Electrical Resistivity and Induced Polarization (IP)

The electrical resistivity and IP data were reduced to apparent resistivities and chargeabilities by fitting a horizontally stratified earth model to the resistivity data or, where both data sets were collected, resistivity and IP simultaneously. A non-linear, least-squares inversion program was used for modeling. This program incorporates the Marquardt procedure (Beck and Arnold, 1977) to calculate new model parameters. The forward routine used in the inversion program is based on the convolution method presented by Koefoed (1972). The parameters solved for in the modeling process are the depth to each layer and resistivities of the layers. The model that provided the lowest standard deviation for all parameters was used as the final interpretation. More confidence can

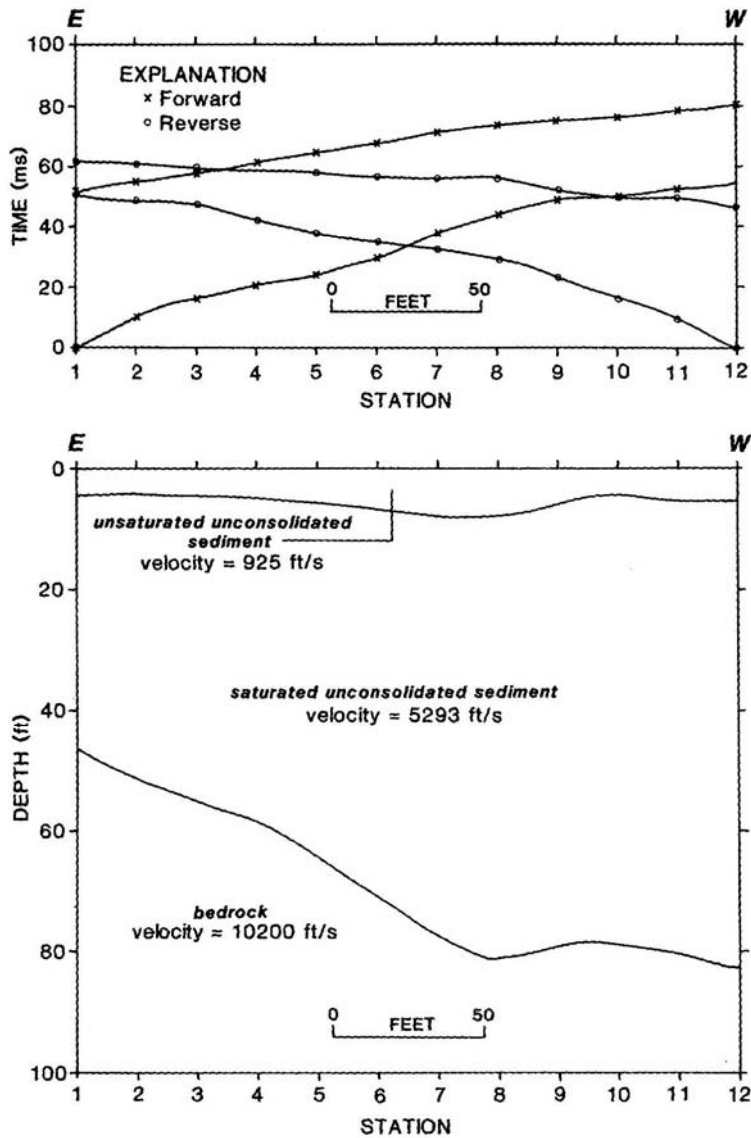


Figure 6. Seismic refraction travel time curve (top) and interpreted cross section (bottom) for line 2.

be placed in the profiles where resistivity and IP data were interpreted simultaneously.

The location, surface elevation, layer number, resistivity, chargeability and depth to top of each layer and geologic interpretation of each of the six electrical soundings are shown in table 2, appendix. All six soundings show a near-surface unsaturated sediment which is 3 to 7 ft thick and has an average resistivity ranging from 29 to 251 ohm-meters. Four electrical soundings were made in Black Meadows swamp. EHVES-1 and EHVES-2 show a low resistivity (15 to 18 ohm-meters), low chargeability (1.8 ms) layer that is about 2 ft thick. This could be an organic-rich

muck. EHVES-3 and EHVES-4 indicate a 5- to 6-ft thick layer of soil mixed with some organic material. Below this layer, soundings in the swamp indicate interbedded clay and sand mixed with clay. The sand mixed with clay has resistivity ranging from 27 to 85 ohm-meters but low chargeabilities (0 to 8 ms). The clays have low resistivities (less than 38 ohm-meters) and low chargeabilities (0 to 2.3 ms).

Bedrock was not detected on soundings EHVES-1 and EHVES-3. A shallow, thick, low-resistivity clay layer made resolution of the deeper, high-resistivity bedrock difficult. The other four soundings show a deep, high-resis-

tivity layer with average resistivities ranging from 128 to 318 ohm-meters. This layer correlated well with bedrock as determined by seismic refraction and well log information.

Figure 7 shows depths, resistivities and chargeabilities for the layers at sounding EHVES-2.

The deepest high-resistivity layer (148 ohm-meters), at a depth of 73 ft, is interpreted as bedrock. The overlying low-resistivity, low-chargeability layer is interpreted as a mixture of sand and clay. The near-surface layer is interpreted as organic-rich muck and unsaturated soil.

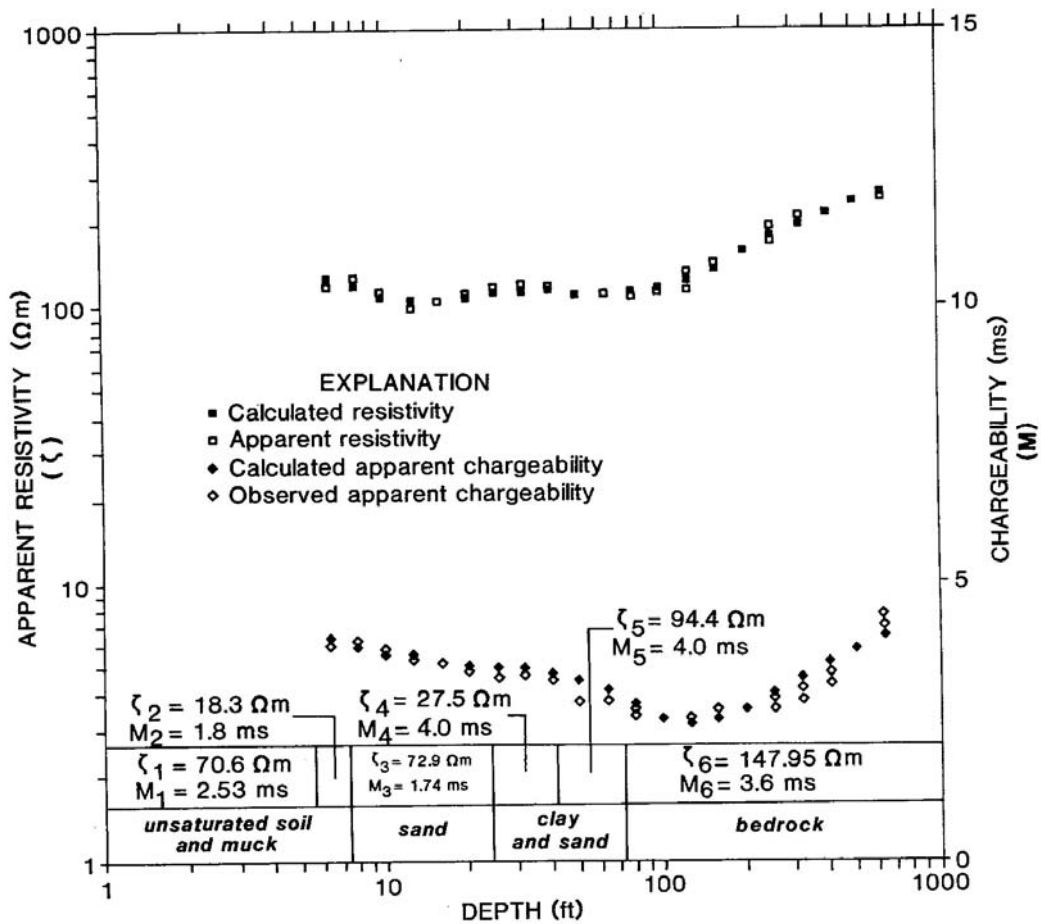


Figure 7. Electrical resistivity-IP sounding EHVES-2 with interpretation.

SUMMARY AND CONCLUSIONS

Lennox and Carlson (1977), Eaton and Watkins (1970), and van Overmeeren (1981) have used combinations of geophysical techniques in ground-water exploration, buried valley studies, or to determine bedrock topography. Hall and Hajnal (1982), Ibrahim and Hinze (1972), and Stewart (1980) have used the gravity method to determine bedrock topography in buried valley

glacial terrains. They have used different interpretive techniques to analyze the gravity data.

In this study we have used data gathered from gravity, seismic refraction, electrical resistivity, and induced polarization surveys, as well as well record data to construct a bedrock topography map (plate III) of the area. This map has been

utilized in ground-water pollution investigations in the East Hanover area (Oudijk, 1987).

The residual gravity data allowed delineation of the East Hanover buried valley and the north-ern extension of the Chatham buried valley.

The western extent of the East Hanover buried valley has been clearly defined by the delineation of a bedrock high along the western boundary of the Morristown Airport. The East Hanover valley appears to trend to the south

from southwestern East Hanover to Florham Park, indicating preglacial drainage to the south. A bedrock low has been inferred in the Birch Hills-Monroe area by gravity interpretation. This bedrock low is beneath 400 ft or more of glacial material and may contain substantial ground water. This bedrock feature needs to be better delineated. Drilling of wells to bedrock, or a detailed gravity survey, is recommended as collection of other geophysical data is hampered by the cultural noise.

REFERENCES

- Beck, J. W., and Arnold, K. J., 1977, Parameter estimation in engineering and science: John Wiley and Sons, Inc., New York, 501 p.
- Bonini, W. E., and Woollard, G. P., 1957, Observational accuracy of high-range geodetic type Worden gravimeters: American Geophysical Union, Transactions, v. 38, p. 147-155.
- Dobrin, M. B., 1976, Introduction to Geophysical Prospecting (3rd ed.): New York, McGraw-Hill, 630 p.
- Eaton, G. P., and Watkins, J. S., 1970, The use of seismic refraction and gravity methods in hydrogeological investigations: in Morley, L. W., Ed., Mining and Ground Water Geophysics: Geological Survey of Canada, Economic Geology Report 26, p. 544- 568.
- Gill, H. E., and Vecchioli, John, 1965, Availability of ground water in Morris County, N. J.: New Jersey Department of Conservation and Economic Development Special Report 25, 56p.
- Gill, H. E., Vecchioli, John, and Bonini, W. E., 1965, Tracing the continuity of Pleistocene aquifers in northern New Jersey by seismic methods: Ground Water, v. 3, no. 4.
- Hall, D. H., and Hajnal, Z., 1962, The gravimeter in studies of buried valleys: Geophysics, v. 27, p.939-951.
- Hoffman, J. L., and Waldner, J. S., 1986, HRASSD: High Resolution Analysis of Shallow Seismic Data, New Jersey Geological Survey Open File Report 86-1, 74p.
- Ibrahim, Abdelwahid, and Hinze, W. J., 1972, Mapping buried bedrock topography with gravity. Ground Water, v. 10, no. 3, p. 18-23.
- James, W R., 1966, FORTRAN IV program using double Fourier series for surface fitting of irregularly spaced data: Computer Contribution 5, State Geological Survey, University of Kansas.
- Kodama, K. P., 1983, Magnetic and gravity evidence for a subsurface connection between the Palisades sill and the Ladentown basalts: Geological Survey of America Bulletin, v. 94, p. 151-158.
- Koefoed, O., 1972, Computation of type curves for electromagnetics: Geophysical Prospecting, v. 20, p. p. 406.
- Lennox, D. H., and Carlson, V., 1967, Geophysical exploration for buried valleys in an area north of Two Hills, Alberta: Geophysics, v. 32, p. 331-362.
- Lyttle, P. T., and Epstein, J. B., 1987, Geologic map of the Newark 1° x 2° quadrangle, New Jersey, Pennsylvania, and New York: U. S. Geological Survey Miscellaneous Investigations Series I-1715 (1:250,000 scale).
- Nichols, W D., 1968, Bedrock topography of eastern Morris and western Essex counties, New Jersey: U. S. Geological Survey Geological Miscellaneous Investigations Map I-549 (scale 1:24,000).
- Olsen, P. E., 1980, Triassic and Jurassic formations of the Newark Basin, in Manspeizer, Warren, ed., Field studies of New Jersey geology and guide to field trips, Annual Meeting of the New York State Geological Assoc. (52nd): Newark, New Jersey, Rutgers University, p. 2-41.
- Oudijk, Gil, 1987, Ground-water contamination and the delineation of a well restriction area in East Hanover Township, Morris County, New Jersey: N. J. Geological Survey Technical Memorandum 87-3, 49p.

- van Overmeeren, R. A., 1981, A combination of electrical resistivity, seismic refraction, and gravity measurements for ground water exploration in Sudan: *Geophysics*, v. 46, p. 1304-1313.
- Salisbury, R. D., 1902, The glacial geology of New Jersey: Geological Survey of New Jersey, Final Report of the State Geologist, v. 5, 802 p.
- Scott, J. H., 1977, SIPT - A seismic refraction inverse modeling program for time-share terminal computer systems: U.S. Geological Survey Open-File Report 77-365.
- Scott, J. H., Tibbetts, B. L., and Bordick, B. G., 1972, Computer analysis of seismic refraction data: U. S. Bureau of Mines 3 Report of Investigations RI 7595.
- Stewart, M. T., 1980, Gravity survey of a deep buried valley: *Ground Water*, v. 18, no. 1, p. 24-30.
- Talwani, M., Worzel, J. L., and Landisman, Mark, 1959, Rapid gravity computations for two-dimensional bodies with application to the Mendocino submarine fracture zones: *Journal Geophysical Research*, v. 64, p. 49-59.
- Ulford, W. M., Geldart, L. P., Sheriff, R. E. and Keys, D. A., 1976, *Applied geophysics*: Cambridge, England, Cambridge University Press, 860 p.
- Vecchioli, John, and Nichols, W. D., 1966, Results of the drought-disaster test-drilling program near Morristown, N. J.: N. J. Department of Conservation and Economic Development Water Resources Circular 16, 48 p.
- Vecchioli, John, Nichols, W. D., and Nemickas, Bronius, 1967, Results of the second phase of the drought-disaster test-drilling program near Morristown, N. J.: N. J. Department of Conservation and Economic Development Water Resources Circular 17, 38 p.

APPENDIX

TABLE 1. Principal facts of gravity stations¹

Sta. no.	Latitude (deg. min.)	Longitude (deg. min.)	Elev. (ft)	Observed gravity (mGal)	TSLGV (mGal)	SBAN (mGal)
EH1	40 47.75	74 27.99	354.80	980198.48	980251.35	-31.59
EH2	40 48.58	74 25.95	309.70	980200.97	980252.58	-33.03
EH3	40 49.13	74 25.13	243.17	980207.34	980253.40	-31.47
EH4	40 49.02	74 24.73	215.05	980209.50	980253.23	-30.83
EH5	40 48.77	74 23.65	182.09	980212.11	980252.86	-29.82
EH6	40 48.92	74 23.32	180.02	980212.47	980253.09	-29.82
EH7	40 47.10	74 25.92	266.47	980203.13	980250.38	-31.26
EH8	40 46.95	74 26.92	365.38	980197.03	980250.15	-31.21
EH9	40 47.68	74 26.92	408.91	980194.18	980251.24	-32.53
EH10	40 47.63	74 26.45	361.98	980197.29	980251.16	-32.16
EH11	40 47.57	74 26.09	290.99	980202.26	980251.08	-31.37
EH12	40 47.56	74 25.95	250.14	980204.84	980251.06	-31.21
EH13	40 47.54	74 25.81	210.82	980207.41	980251.04	-30.98
EH14	40 47.53	74 25.67	198.27	980208.11	980251.01	-31.01
EH15	40 47.51	74 25.53	186.74	980208.67	980250.99	-31.12
EH16	40 47.50	74 25.39	182.84	980208.78	980250.97	-31.21
EH17	40 47.48	74 25.25	180.80	980208.77	980250.94	-31.33
EH18	40 47.46	74 25.11	180.18	980208.68	980250.92	-31.43
EH19	40 47.45	74 24.97	180.18	980208.64	980250.90	-31.45
EH20	40 47.43	74 24.83	179.99	980208.49	980250.87	-31.59
EH21	40 47.42	74 24.68	200.72	980207.13	980250.85	-31.68
EH22	40 47.40	74 24.55	226.13	980205.17	980250.83	-32.09
EH23	40 47.39	74 24.40	192.02	980207.73	980250.80	-31.56
EH24	40 47.37	74 24.26	181.43	980208.42	980250.78	-31.48
EH25	40 47.36	74 24.12	183.02	980208.54	980250.76	-31.25
EH26	40 47.34	74 23.98	200.57	980207.32	980250.74	-31.39
EH27	40 47.33	74 23.84	207.13	980207.09	980250.72	-31.21
EH28	40 47.31	74 23.70	198.24	980207.90	980250.70	-30.90
EH29	40 47.30	74 23.56	189.03	980208.55	980250.67	-30.78
EH30	40 47.34	74 23.39	193.53	980208.26	980250.74	-30.87
EH31	40 47.78	74 27.56	380.72	980196.86	980251.39	-31.69
EH32	40 48.01	74 27.05	389.83	980195.29	980251.72	-33.06
EH33	40 48.34	74 26.79	312.49	980200.28	980252.22	-33.20
EH34	40 48.48	74 26.49	289.67	980201.95	980252.44	-33.11
EH35	40 48.21	74 26.03	231.43	980206.04	980252.03	-32.10
EH36	40 47.91	74 26.03	252.99	980204.57	980251.59	-31.84
EH37	40 47.98	74 26.69	401.34	980194.51	980251.69	-33.10
EH38	40 47.93	74 26.93	408.33	980194.07	980251.62	-33.06
EH39	40 48.20	74 26.46	316.71	980200.23	980252.01	-32.79
EH40	40 47.89	74 26.32	312.11	980200.58	980251.55	-32.25
EH41	40 48.78	74 25.74	282.50	980203.30	980252.87	-32.63
EH42	40 48.95	74 25.57	248.29	980206.52	980253.13	-31.72
EH43	40 49.20	74 24.97	232.23	980208.52	980253.50	-31.05
EH44	40 49.30	74 24.74	193.95	980211.55	980253.65	-30.47
EH45	40 49.27	74 24.60	192.41	980211.72	980253.60	-30.34

¹Density = 2.670 g/cc; Theoretical Sea-level Gravity (TSLGV) based on 1930 International Gravity Formula; Principal gravity base station at Princeton University (Bonini and Woollard, 1957): Observed gravity = 980177.6 mGal; SBAN: Simple Bouguer Anomaly

TABLE 1. cont.

Sta. no.	Latitude (deg. min.)	Longitude (deg. min.)	Elev. (ft)	Observed gravity (mGal)	TSLGV (mGal)	SBAN (mGal)
E446	40 49.22	74 24.47	203.47	980210.96	980253.53	-3037
EH47	40 49.15	14 24.37	201.70	980211.18	980253.42	-30.15
EH48	40 49.07	74 24.27	191.97	980211.78	980253.31	-30.02
EH49	40 49.01	74 24.16	183.89	980212.06	980253.21	-30.13
EHSO	40 48.93	74 24.05	181.30	980212.05	980253.11	-30.19
EH51	40 48.87	74 23.95	182.36	980211.78	980253.01	-30.29
EH52	40 48.80	74 23.80	181.14	980212.02	980252.91	-30.03
EH53	40 48.72	74 23.43	224.31	980209.11	980252.79	-30.24
EH54	40 48.69	74 23.30	222.18	980209.40	980252.74	-30.02
EH55	40 48.65	74 23.16	217.46	980209.64	980252.68	-30.00
EH56	40 48.61	74 23.03	21333	980210.00	980252.62	-29.83
EH57	40 48.56	74 22.90	209.00	980210.23	980252.56	-29.80
EH58	40 49.51	74 25.22	217.13	980210.06	980253.96	-30.89
EH59	40 49.46	74 25.10	208.80	980210.31	980253.89	-31.05
EH60	40 49.39	74 25.00	205.58	980210.68	980253.78	-30.77
EH61	40 49.34	74 24.87	199.48	980211.09	980253.70	-30.66
EH62	40 48.59	74 23.64	190.50	980211.25	980252.60	-29.92
EH63	40 48.33	74 23.66	204.11	980209.54	980252.20	-30.42
EH64	40 48.12	74 23.67	232.07	980207.17	980251.90	-30.82
EH65	40 47.92	74 23.60	219.24	980207.49	980251.59	-30.96
EH66	40 47.71	74 23.42	214.30	980207.49	980251.28	-30.94
EH67	40 47.38	74 23.36	191.51	980208.69	980250.79	-30.61
EH68	40 47.39	74 27.29	379.80	980196.91	980250.81	-31.12
EH69	40 47.55	74 27.08	389.74	980195.84	980251.04	-31.83
EH70	40 47.31	74 26.04	317.10	980200.14	980250.69	-31.53
EH71	40 46.99	74 26.34	373.49	980196.31	980250.21	-31.50
EH72	40 48.68	74 24.95	190.50	980210.45	980252.73	-30.86
EH73	40 48.77	74 25.10	196.76	980209.81	980252.86	-31.25
EH74	40 48.93	74 24.08	231.49	980207.95	980253.10	-31.27
EH75	40 48.85	74 24.98	200.59	980210.09	980252.98	-30.86
EH76	40 47.97	74 25.32	201.15	980208.63	980251.67	-30.98
EH77	40 48.62	74 25.62	262.72	980204.69	980252.63	-32.19
EH78	40 48.68	74 25.30	203.48	980209.00	980252.73	-31.53
EH79	40 48.47	74 25.75	302.59	980201.64	980252.41	-32.63
EH80	40 48.38	74 25.47	266.17	980204.06	980252.29	-32.27
EH81	40 49.60	74 24.90	258.21	980207.60	980254.10	-31.01
EH82	40 49.79	74 24.73	269.21	980207.61	980254.38	-30.63
EH83	40 50.03	74 24.50	248.59	980209.74	980254.74	-30.09
EH84	40 50.30	74 24.50	21937	980212.02	980255.14	-29.97
EH85	40 50.08	74 24.10	231.16	980211.20	980254.81	-29.76
EH86	40 49.83	74 23.67	195.78	980212.98	980254.44	-29.72
EH87	40 49.70	74 23.90	239.26	980209.98	980254.24	-29.91
EH88	40 49.85	74 24.12	230.78	980210.79	980254.47	-29.84
EH89	40 49.12	74 24.17	277.85	980206.67	980253.38	-30.04
EH90	40 49.77	74 24.37	242.52	980209.59	980254.34	-30.21

Density = 2.670 g/cc; Theoretical Sea-level Gravity (TSLGV) based on 1930 International Gravity Formula; Principal gravity base station at Princeton University (Bonini and Woollard, 1957); Observed gravity = 980177.6 mGal; SBAN: Simple Bouguer Anomaly

TABLE 1. cont.

Sta. no.	Latitude (deg. min.)	Longitude (deg. min.)	Elev. (ft)	Observed gravity (mGal)	TSLGV (mGal)	SBAN (mGal)
EH91	4049.45	7424.32	248.21	980208.41	980253.87	-30.58
EH92	4049.55	7424.70	236.33	980209.17	980254.02	-30.68
EH93	4049.69	7424.53	252.41	980208.82	980254.23	-30.27
EH94	4049.33	7424.95	198.48	980212.07	980253.70	-29.73
EH95	4049.52	7423.68	216.23	980211.05	980253.97	-29.96
EH96	4049.63	7423.45	186.96	980213.39	980254.14	-29.55
EH97	4048.96	7423.65	195.07	980212.45	980253.15	-29.01
EH98	4048.75	7423.62	184.23	980212.63	980252.83	-29.15
EH99	4049.50	7423.08	173.91	980213.90	980253.95	-29.62
EH100	4049.50	7422.82	178.50	980213.92	980253.95	-29.33
EH101	4049.52	7422.45	188.55	980213.52	980253.97	-29.15
EH102	4049.23	7422.33	198.51	980212.51	980253.55	-29.13
EH103	4049.05	7422.97	189.14	980212.38	980253.28	-29.56
EH104	4048.90	7423.27	180.50	980212.69	980253.05	-29.54
EH105	4048.17	7423.95	179.09	980210.62	980251.96	-30.60
EH106	4048.00	7423.85	180.78	980210.14	980251.72	-30.73
EH107	4047.81	7423.75	197.62	980208.90	980251.43	-30.69
EH108	4047.58	7423.65	185.67	980209.03	980251.10	-30.93
EH109	4047.47	7423.93	193.54	980208.04	980250.92	-31.28
EH110	4047.60	7424.12	181.60	980209.03	980251.12	-31.20
EH111	4047.82	7424.18	192.77	980208.46	980251.44	-31.42
EH112	4047.62	7424.80	180.33	980208.67	980251.15	-31.67
EH113	4047.82	7424.37	178.58	980209.01	980251.44	-31.72
EH114	4048.05	7424.23	178.96	980209.71	980251.79	-31.35
EH115	4047.82	7425.18	181.57	980208.82	980251.44	-31.74
EH116	4048.04	7421.56	177.32	980212.42	980251.78	-28.73
EH117	4048.85	7422.70	203.09	980211.43	980252.98	-29.38
EH118	4047.57	7425.15	180.92	980208.60	980251.07	-31.62
EH119	4047.72	7425.02	182.53	980208.80	980251.29	-31.55
EH120	4047.80	7424.93	182.64	980208.88	980251.42	-31.58
EH121	4047.78	7424.58	180.94	980208.99	980251.39	-31.54
EH122	4048.12	7424.64	181.14	980209.64	980251.89	-31.39
EH123	4048.13	7424.65	180.70	980210.01	980251.91	-31.07
EH124	4048.40	7424.49	180.35	980210.42	980252.31	-31.08
EH125	4048.72	7424.12	178.12	980211.63	980252.78	-30.47
EH126	4048.55	7424.27	178.74	980211.26	980252.53	-30.55
EH127	4047.97	7424.93	177.55	980209.39	980251.67	-31.64
EH128	4048.01	7425.30	183.38	980209.13	980251.73	-31.60
EH129	4048.07	7425.49	186.05	980209.09	980251.82	-31.57
EH130	4047.70	7425.26	182.31	980208.60	980251.27	-31.74
EH131	4047.68	7425.80	197.24	980208.15	980251.24	-31.26

Density = 2.670 g/cc; Theoretical Sea-level Gravity MLGV) based on 1930 International Gravity Formula; Principal gravity base station at Princeton University (Bonini and Woollard,1957); Observed gravity = 980177.6 mGal; SBAN: Simple Bouguer Anomaly

Table 2. Seismic refraction field parameters and interpretations.

Sta. no.	Location (lat./long., deg., min., sec)	Elev. (ft)	Geophone spacing (ft)	Shot point location	Layer	Depth to top of layer (ft) at geophone no.			Layer velocity (ft/s)	Interpretation
						1	6	12		
EH1	40 48 30 74 25 11	200	50	1. At geophone 1	1				4290	Sat. zone
				2. midpoint between geophone 6 and 7	2	36	23	46	13176	Bedrock (shale)
				3. At geophone 12						
EH2	40 48 52 74 24 02	190	20	1. 200 ft from geophone 1	1				925	Unsat. zone
				2. At geophone 1	2	4	6	5	5293	Sat. zone
				3. At geophone 12	3	46	71	83	10200	Bedrock
				4. 200 ft from geophone 12						
EH3	40 49 05 74 23 37	180	20	1. 300 ft from geophone 1	1				974	Unsat. zone
				2. 200 ft from geophone 1	2	5	9	15	6115	Sat. zone
				3. At geophone 1	3	114	108	117	11661	Bedrock
				4. At geophone 12						
				5. 200 ft from geophone 12						
EH4	40 47 52 74 24 23	180	20	1. 198 ft from geophone 1	1				1430	Unsat. zone
				2. At geophone 1	2	11	10	9	5594	Sat. zone
				3. At geophone 12	3	92	93	90	11707	Bedrock
				4. 198 ft from geophone 12						
EH5	40 50 02 74 23 39	215	20	1. 200 ft from geophone 1	1				1236	Unsat. zone
				2. At geophone 1	2	9	9	10	7235	Saturated
				3. At geophone 12	3	73	78	78	13631	Bedrock
				4. 200 ft from geophone 12						
EH6	40 48 52 74 24 37	195	20	1. 200 ft from geophone 1	1				2187	Unsat. zone
				2. At geophone 1	2	8	10	12	6976	Sat. zone
				3. At geophone 12	3	38	36	51	12660	Bedrock
				4. 200 ft from geophone 12						
EH7	40 48 28 74 24 50	190	20	1. 200 ft from geophone 1	1				1485	Unsat. zone
				2. At geophone 1	2	12	11	11	6011	Sat. zone
				3. At geophone 12	3	42	72	85	16005	Bedrock
EH8	40 47 38 74 24 39	180	20	1. 300 ft from geophone 1	1				1227	Unsat. zone
				2. 200 ft from geophone 1	2	10	8	9	5937	Sat. zone
				3. At geophone 1	3	79	102	121	13625	Bedrock
				4. At geophone 12						
				5. 200 ft from geophone 12						

Table 2. (cont.)

Sta. no.	Location (lat./long, deg., min., sec.)	Elev. (ft)	Geophone spacing (ft)	Shot point location	Layer	Depth to top of layer (ft) at geophone no.			Layer velocity (ft/s)	Interpretation	
						1	6	12			
EH9	40 47 56 74 24 47	190	20	1. 200 ft from geophone 1	1				1533	Unsat. zone	
				2. At geophone 1	2	13	12	10	5769	Sat. zone	
				3. At geophone 12	3	58	65	57	14335	Bedrock	
				4. 200 ft from geophone 12							
EH10	40 48 55 74 24 24	190	20	1. 200 ft from geophone 1	1				1408	Unsat. zone	
				2. At geophone 1	2	8	10	8	6773	Sat. zone	
				3. At geophone 12	3	52	43	41	12501	Bedrock	
				4. 200 ft from geophone 12							
EH11	40 48 19 74 24 24	180	20	1. 200 ft from geophone 1	1				1229	Unsat. zone	
				2. At geophone 1	2	11	14	22	6418	Sat. zone	
				3. At geophone 12	3	94	88	56	12105	Bedrock	
				4. 200 ft from geophone 12							
EH12	40 48 38 74 24 08	180	20	1. 200 ft from geophone 1	1				1099	Unsat. zone	
				2. At geophone 1	2	5	8	8	5384	Sat. zone	
				3. At geophone 12	3	115	112	109	12433	Bedrock	
				4. 200 ft from geophone 12							
EH13	40 48 55 74 25 17	250	20	1. 300 ft from geophone 1	1				2460	Unsat. zone	
				2. 200 ft from geophone 1	2	59	54	47	7467	Sat. zone	
				3. At geophone 1	3	145	129	128	13726	Bedrock	
				4. At geophone 12							
				5. 200 ft from geophone 12							
				6. 300 ft from geophone 12							
EH14	40 48 43 74 24 47	205	20	1. 200 ft from geophone 1	1				1000	Unsat. zone	
				2. 140 ft from geophone 12	2	13	2	10	5000	Sat. zone	
				3. At geophone 1	3		48	30	10,000	Bedrock	
				4. At geophone 12							
EH15	40 48 03 74 25 33	195	20	1. 200 ft from geophone 1	1				2330	Unsat. zone	
				2. 140 ft from geophone 12	2	14	14	15	8386	Sat. zone	
				3. At geophone 1	3	72	81	88	14169	Bedrock	
				4. At geophone 12							

Table 2. (cont.)

Sta. no.	Location (lat./long., deg., min., sec.)	Elev. (ft)	Geophone spacing (ft)	Shot point location	Layer	Depth to top of layer (ft) at geophone no.			Layer velocity (ft/s)	Interpretation
						1	6	12		
EH16	40 48 14 74 25 26	210	20	1. 200 ft from geophone 1	1				1301	Unsat. zone
					2	8	7	7	7927	Sat. zone
				2. 300 ft from geophone 12	3	45	65	63	11906	Bedrock
				3. At geophone 1						
				4. At geophone 12						
EH17	40 48 14 74 25 26	210	20	1. 180 ft from geophone 1	1				1280	Unsat. zone
					2	6	8	6	7768	Saturated
				2. 180 ft from geophone 12	3	45	65	63	13631	Bedrock
				3. At geophone 1						
				4. At geophone 12						
EH18	40 48 10 74 25 52	230	20	1. 180 ft from geophone 1	1				5478	Sat. zone
					2	16	12	4	7160	
				2. 180 ft from geophone 12	3	50	58	64	10626	Bedrock
				3. At geophone 1						
				4. At geophone 12						
EH20	40 50 09 74 25 06	280	20	1. 200 ft from geophone 1	1				1214	Unsat. zone
				2. 100 ft from geophone 1	2	6	6	8	5571	Sat. zone
				3. midpoint between geophone 6 and 7	3	61	70	54	10463	Bedrock
				4. 100 ft from geophone 12						
				5. 200 ft from geophone 12						
EH21	40 49 59 74 24 11	250	20	1. 200 ft from geophone 1	1				2028	Unsat. zone
				2. 100 ft from geophone 1	2	12	18	11	3851	Sat. zone
				3. midpoint between geophones 6 and 7	3	97	99	114	13782	Bedrock
				4. 100 ft from geophone 12						
				5. 175 ft from geophone						
EH22	40 44 31 74 25 15	270	20	1. 100 ft from geophone 1	1				2033	Unsat. zone.
					2	17	19	9	7130	Sat. zone
				2. 10 ft from geophone 1	3	130	137	102	10638	Bedrock
				3. midpoint between geophone 6 and 7						
				4. 31 ft from geophone 12						
				5. 200 ft from geophone 12						
EH23	40 49 32 74 23 11	170	20	1. 200 ft from geophone 1	1				1413	Unsat. zone
				2. 100 ft from geophone 1	2	13	8	11	5245	Sat. zone
				3. midpoint between geophones 6 and 7	3	43	65	67	12924	Bedrock
				4. 100 ft from geophone 12						
				5. 200 ft from geophone 12						

TABLE 3. Electrical Resistivity and IP interpretations

Line no., location (lat./long.)	Elev. (ft)	Layer no.	Resistivity (ohm-m)	Chargeability M (ms)	Depth to top (ft)	Interpretation
EHVES-1 40 47 55 74 24 24	190.	1	251.	...		Unsat. soil
		2	15.5	...	3.2	Muck
		3	16.2	...	5.4	"
		4	38.	...	31.6	Clay & sand
		5	9.3	...	101.5	Clay
EHVES-2 40 48 57 74 24 07	190.	1	70.6	2.53		Unsat. soil
		2	18.3	1.8	4.6	Muck
		3	72.9	1.74	6.7	Sand
		4	27.5	4.02	26.1	Clay & sand
		5	44.4	4.56	41.9	"
		6	148.	3.61	73.1	Bedrock
EHVES-3 40 48 27 74 25 18	200.	1	29.4	0.96		Unsat. soil
		2	78.8	2.02	5.5	Sand
		3	79.0	6.01	25.3	Sand
		4	38.	2.3	80.	Clay
		5	69.7	6.9	164.6	Clay & sand
EHVES-4 40 49 01 74 23 34	190.	1	53.	2.0		Unsat. soil
		2	30.6	0.7	4.9	Muck
		3	73.8	2.1	9.8	Sand & clay
		4	65.8	0.8	37.5	"
		5	23.8	0.	63.0	Clay
		6	191.4	4.14	91.0	Bedrock
EHVES-5 40 48 55 74 24 36	190.	1	82.	...		Unsat. soil
		2	61.0	...	7.0	Clay & sand
		3	119.0	...	26.4	Bedrock
EHVES-6 40 50 02 74 23 41	205.	1	145.0	...		Unsat. soil
		2	22.0	...	4.8	Sat. soil
		3	84.9	...	13.3	Sand & clay
		4	14.3	...	78.6	Clay
		5	318.0	...	107.7	Bedrock

Table 4. Record of wells (from Bureau of Water Allocation)

Well no.	Permit no.	Surface elevation (ft)	Bedrock elevation (ft)	Well no.	Permit no.	Surface elevation (ft)	Bedrock elevation (ft)
1	17435	290	180				
4	13904	285	205	27	8413	200	120
5	13414	200	78	28	8562	190	125
6	25562	294	154	29	11209	200	110
7	21923	280	165	30	7639	200	110
8	21574	210	118	31	14873	200	75
9	3527	270	126	32	13475	195	135
10	11204	265	122	34	20501	195	65
12	13420	280	200	35	11330	196	100
13	8517	180	95	36	11341	190	80
14	7655	180	100	37	14092	345	195
15	9973	180	95	38	15756	300	125
16	8954	270	190	39	19279	378	138
17	21078	260	170	41	8244	205	125
19	10748	250	155	42	5647	340	200
20	22516	190	100	43	8577	345	200
21	13563	235	134	44	22128	370	105
22	11115	190	110	45	15313	390	162
23	13875	190	120	47	22128	370	125
24	11569	190	130	48	9086	175	105
25	9900	185	122	49	11968	380	187



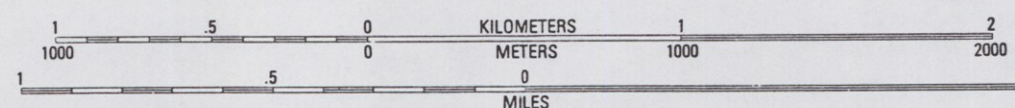
PLATE 1. BOUGUER GRAVITY ANOMALY MAP

Base from U.S. Geological Survey
 Caldwell 1981, Morristown 1981

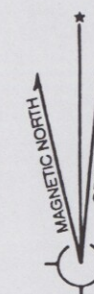
EXPLANATION

- 31.0 Gravity contour - contour interval 0.5 mGal
- 23 Gravity station - refer to Table 1

Scale 1:24,000



Base Map Contour Interval 20 Feet
 National Geodetic Vertical Datum of 1929



STUDY AREA



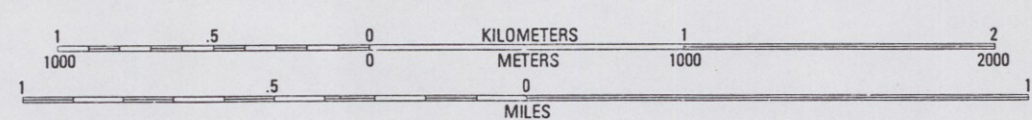
PLATE 2. RESIDUAL GRAVITY MAP

Base from U.S. Geological Survey
 Caldwell 1981, Morristown 1981

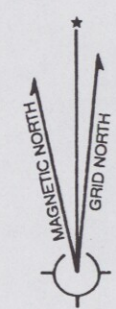
EXPLANATION

- 0.25 — Gravity contour - contour interval 0.25 mGal
- 23. Gravity station - refer to Table 1

Scale 1:24,000



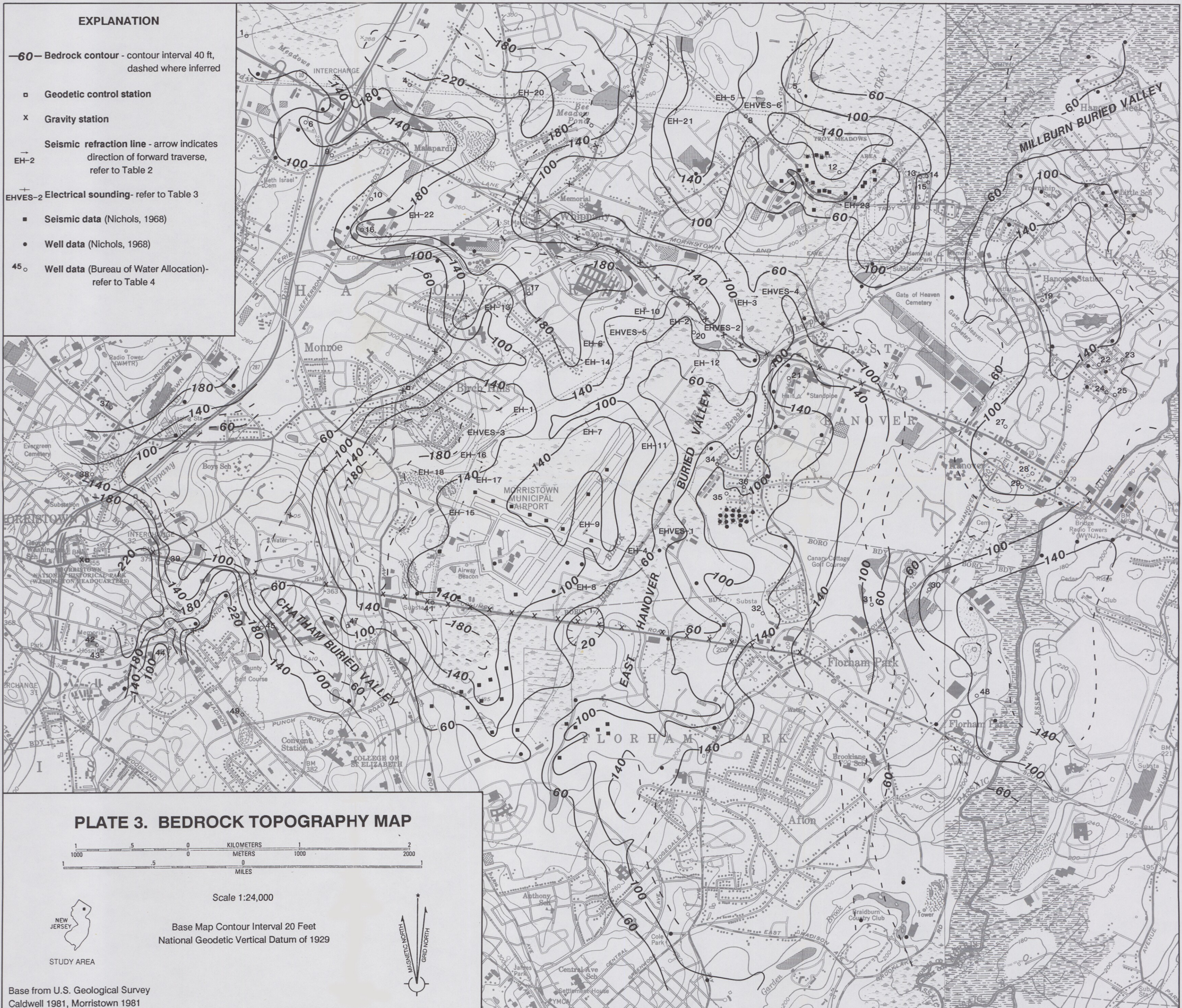
Base Map Contour Interval 20 Feet
 National Geodetic Vertical Datum of 1929



STUDY AREA

74° 28' 30"
 40° 50' 30"

74° 21'
 40° 50' 30"



EXPLANATION

- 60— Bedrock contour - contour interval 40 ft, dashed where inferred
- Geodetic control station
- x Gravity station
- Seismic refraction line - arrow indicates direction of forward traverse, refer to Table 2
- EH-2
- +EHVES-2 Electrical sounding- refer to Table 3
- Seismic data (Nichols, 1968)
- Well data (Nichols, 1968)
- 45° Well data (Bureau of Water Allocation)- refer to Table 4



PLATE 3. BEDROCK TOPOGRAPHY MAP

1 5 0 1 2
 1000 5000 10000 20000
 KILOMETERS
 METERS
 0 5 1
 MILES

Scale 1:24,000

Base Map Contour Interval 20 Feet
 National Geodetic Vertical Datum of 1929

NEW JERSEY
 STUDY AREA

Base from U.S. Geological Survey
 Caldwell 1981, Morristown 1981

MAGNETIC NORTH
 GRID NORTH

40° 45'
 74° 28' 30"

40° 45'
 74° 21'

Geophysical Investigations to Determine Bedrock Topography in the East Hanover-Morristown Area, Morris County, New Jersey
(New Jersey Geological Survey, Geological Survey Report 17)

ISSN 0741-7357

GEOPHYSICAL INVESTIGATIONS TO
Your Price \$ 10.00



GSR 17